



HAL
open science

The role of the secondary fluorophore in ternary plastic scintillators aiming at discriminating fast neutrons from gamma-rays

Eva Montbarbon, Zhengyu Zhang, Amélie Grabowski, Romuald Woo, Dominique Tromson, Chrystèle Dehé-Pittance, Robert Bernard Pansu, Guillaume H. V. Bertrand, Matthieu Hamel

► To cite this version:

Eva Montbarbon, Zhengyu Zhang, Amélie Grabowski, Romuald Woo, Dominique Tromson, et al.. The role of the secondary fluorophore in ternary plastic scintillators aiming at discriminating fast neutrons from gamma-rays. *Journal of Luminescence*, 2019, 213, pp.67-74. 10.1016/j.jlumin.2019.04.059 . hal-02325687

HAL Id: hal-02325687

<https://hal.science/hal-02325687>

Submitted on 23 Oct 2019

HAL is a multi-disciplinary open access archive for the deposit and dissemination of scientific research documents, whether they are published or not. The documents may come from teaching and research institutions in France or abroad, or from public or private research centers.

L'archive ouverte pluridisciplinaire **HAL**, est destinée au dépôt et à la diffusion de documents scientifiques de niveau recherche, publiés ou non, émanant des établissements d'enseignement et de recherche français ou étrangers, des laboratoires publics ou privés.

The role of the secondary fluorophore in ternary plastic scintillators aiming at discriminating fast neutrons from gamma-rays

1

Eva Montbarbon^{a, b}, Zhengyu Zhang^b, Amélie Grabowski^a, Romuald Woo^a, Dominique Tromson^a,
Chrystèle Dehé-Pittance^a, Robert B. Pansu^b, Guillaume H. V. Bertrand^a, Matthieu Hamel^{a, *}

2 ^a CEA, LIST, Laboratoire Capteurs et Architectures Électroniques, F-91191 Gif-sur-Yvette Cedex,
3 France.

4 ^b ENS Paris Saclay, UMR CNRS 8531, F-94235 Cachan, France.

5

6 Abstract

7 Since Helium-3 shortage announcement, organic scintillators play a major role in neutron detection.
8 Our laboratory decided to focus on plastic scintillators and their ability to discriminate fast neutrons
9 from gamma rays. In this work, we highlight the influence of the secondary fluorophore in lab-made
10 plastic scintillators. The secondary fluorophore is generally added in the scintillating mixture to shift
11 the emission wavelength towards the transparency domain of the material to improve its attenuation
12 length. Thus, it is considered as a harmless molecule and is barely seen as a key criterion that could
13 enhance the performances of the organic scintillator. In our work, we demonstrate that this molecule,
14 even added at a small concentration (typically in the range 0.02 – 0.2 wt%), directly impacts the
15 neutron/gamma discrimination ability of plastics. Not only the secondary fluorophore plays a role in
16 self-absorption of the scintillating material, but also the couple it creates with the primary fluorophore
17 has to be carefully chosen, as some specific triplet energy transfers between the two fluorophores can
18 influence the neutron/gamma discrimination abilities of the plastic scintillator. Aside from classical
19 photophysical inconveniences such as self-absorption or diffusion, the possibility that the whole, bulk
20 material was heterogeneous in a photochemical point of view was also checked. Thus, various samples
21 were cut from bulk monoliths and their pulse shape discrimination compared with the parent
22 scintillator in terms of Figure of Merit and light output.

23

24 Keywords

25 n/γ discrimination; plastic scintillators; secondary fluorophore; self-absorption; triplet-triplet
26 annihilation.

27

28 Highlights

- 29 • Fast neutrons/gamma discrimination efficiency is usually reduced when the volume of a
30 plastic scintillator is increased.
- 31 • This effect is studied, first in a morphologically way, then chemically and photophysically.

32

33

I. INTRODUCTION

34

35 Protection of civilians and facilities against CBRN-E threats (“Chemical, Biological, Radiological,
36 Nuclear, and Explosive” threats) has become a true challenge these last fifteen years. In the context of
37 nuclear and radiological threats, Helium-3 based counters have proven their efficiency and are
38 considered as the “Gold standard” in neutron detection. These historical detectors are widely used in
39 Radiation Portal Monitors (RPMs) which are installed, *e.g.*, at borders and tolls. However, the shortage
40 of Helium-3 production which occurred for years have incited many scientists to imagine reliable and
41 potentially cheaper alternatives.^{1,2}

42 In this situation, organic scintillators may pave the way to a new paradigm in neutron detection.
43 Indeed, some scintillators were chemically engineered for Pulse Shape Discrimination (PSD), and
44 especially the discrimination between fast neutrons and gamma rays, which falls within nuclear and
45 radiological detection.³ Organic crystals are among the best performing materials to discriminate fast
46 neutrons from gamma rays but are constrained to high-price, small-scale samples. Contrary to crystals,
47 liquid and plastic scintillators have the benefit of being cheap, scalable to sizes fully compatible with
48 sensors encountered in RPMs and easy to manufacture. Thus, they could be suitable to replace ³He
49 counters, owing to the fact they are good enough to meet normative neutron detection requirements.

50 A plastic scintillator is generally made out of a polymer matrix, a primary and a secondary fluorophore.
51 The first fluorophore collects the singlet and triplets produced by the ionizing particle in the material.
52 Its concentration is chosen to allow the presence of a delayed fluorescence from triplet-triplet
53 annihilation (TTA). This TTA probability is higher in the case of fast neutrons compared to gamma rays.
54 The secondary fluorophore absorbs the first fluorophore’s emission and acts as a “wavelength shifter”
55 by emitting light at wavelengths that are in the transparency domain of the plastic scintillator, and for

56 which the photon to electron conversion is the highest according to standard photocathodes used in
57 photomultiplier tubes (most of the time $\lambda \approx 420$ nm).

58 Generally, the secondary fluorophore is mainly being considered as a wavelength shifter. The nature
59 of the molecule and its concentration is not considered to influence *a priori* the neutron/gamma
60 discrimination abilities of the plastic scintillator in which it is incorporated. The results described herein
61 show that this postulate must be reconsidered. Our aim is to analyze the main photophysical
62 phenomena of the discrimination between fast neutrons and gamma rays in plastic scintillators, and
63 especially the role of the secondary fluorophore in this process. For this purpose, different experiments
64 have been carried out and are presented in the following.

65 For this purpose, the influence of the secondary fluorophore was demonstrated towards the
66 performances of the scintillator, and the photophysical processes involving this molecule were
67 evidenced. The first experiment consisted in highlighting the influence of the secondary fluorophore
68 on the neutron/gamma discrimination properties. In this purpose, a set of eight plastic scintillators of
69 the same volume has been synthesized. Four different secondary fluorophores were tested: bis-
70 methylstyrylbenzene (bis-MSB), 9,10-diphenylanthracene (9,10-DPA), 1,4-bis(5-phenyl-2-
71 oxazolyl)benzene (POPOP) and 1,4-bis-2-(4-methyl-5-phenyloxazolyl)benzene (diMePOPOP). The
72 scintillators were intentionally prepared in pairs, the weight concentration of the introduced
73 secondary fluorophore being either 0.1 or 0.2 wt%. The results of the eight plastic samples were
74 presented in terms of FoM, scintillation decay time and relative intensities. The FoM was evaluated
75 thanks to Equation 1, where μ_n and μ_γ are the mean positions of the neutron and the gamma ray
76 contributions, and σ_n and σ_γ are the standard deviations of neutron and gamma lobes:

77 *Equation 1*

$$78 \quad FoM = \frac{|\mu_n - \mu_\gamma|}{2.35(\sigma_n^2 + \sigma_\gamma^2)}$$

79 The next experiment consisted in slide-cutting two of these plastic samples, centimeter by centimeter.
80 In this way, we could evaluate the Figure of Merit value (FoM) as a function of the length of the plastic
81 material.

82 In addition, experiments related with the homogeneity of large or long PSD-plastic were conducted,
83 where portions were randomly isolated from bulk scintillators. The obtained results enabled us to
84 propose two assumptions of the FoM differences we notice: the formation of exciplexes in the sample,
85 or triplet energy transfers between the primary and the secondary fluorophores. The last part of this
86 paper describes experiments we carried out to verify these hypotheses. Finally, conclusions about
87 photophysical phenomena were drawn.

88 Since the 70's, almost two decades after the discovery of plastic scintillators, it has been observed that
89 the observed light yield and the discriminating abilities of organic scintillators decrease when the

90 volume increases. For instance, Kalyna and Taylor carried out fast neutrons/gamma rays discrimination
91 experiments with liquid scintillators of different diameter but with a constant height, which was stand
92 equal to 1 inch.⁴ The authors observe that the FoM of a 4" Ø NE213 liquid scintillator is equal to 1.75,
93 whereas it only reaches 0.9 when its diameter is doubled. According to them, this difference of FoM
94 value is mainly due to the high voltage of the photomultiplier tube (PMT) which is applied, and has to
95 be adjusted according to the dimensions of the scintillator. Sipp and Miehe compare the
96 radioluminescence decays of BIBUQ-based fluorescent solutions (BIBUQ stands for 4,4'-bis-(2-butyl-
97 octyloxy)-*p*-quaterphenyl), in which 56 g.L⁻¹ BIBUQ is incorporated in xylene.⁵ 0.2, 1 and 5 cm-long
98 optical length cuvettes are thus being compared. A sum of two exponential functions is used to fit the
99 measured decay times. The prompt decay of these liquid scintillators, which is relative to fast
100 fluorescence, varies very slightly from one solution to another. However, the Full Width at Half
101 Maximum (FWHM) of the recorded pulses increases from 1.58 ns up to 2.28 ns when the optical length
102 cuvette is increased from 0.2 cm up to 5 cm. According to Sipp and Miehe, this time difference is due
103 to an absorption phenomenon, where scintillation photons are self-absorbed by the material and
104 reemitted with a second delay. Moszyński *et al.* evaluated the neutron/gamma discrimination abilities
105 of NE213 with different volumes. With their detection setup, they notice that the FoM is equal to 1.58
106 at 300 keVee for this liquid scintillator when its dimensions are 16 cm diameter and 20 cm height,
107 whereas the FoM reaches 2.61 when the same scintillator measures 5 cm diameter and 5 cm height.⁶
108 In conclusion, the authors explain this loss of luminous and discriminating signals of organic materials
109 by self-absorption. As the PSD is based on very subtle differences in the decay time distributions
110 between a gamma and a neutron interaction within the material, self-absorption phenomenon tends
111 to fade out this small discrepancy. Recently, the impact of the secondary dye – both in terms of light
112 output and FoM – was experimentally observed on neutron/gamma discriminating plastics, but not
113 explained.⁷ Also, the POPOP molecule suffered from important irradiation doses to give a derivative.⁸
114 Despite the fact that the scintillator showed a degraded light output, the FoM value was improved.
115 As a reminder, self-absorption is a molecular absorption phenomenon that takes place inside the
116 scintillator: scintillation photons are emitted, possibly reabsorbed by the material, and then reemitted
117 by secondary emission. Thus, the larger the volume, the more self-absorption may occur. In a ternary
118 system, self-absorption is due to a spectral overlap between the absorption and the emission spectra
119 of the last fluorophore, thus the secondary fluorophore. Besides, the Stokes shift quantifies this
120 overlap. Equation 2 gives the formula of the Stokes shift $\Delta\nu_{Stokes}$:

121

122 *Equation 2*

123

$$\Delta\nu_{Stokes} = \nu_{abs} - \nu_{fluor} = 1/\lambda_{abs} - 1/\lambda_{fluor}$$

124 ν_{abs} and ν_{fluo} are respectively the wavenumbers of absorbance and fluorescence (in cm^{-1}).
125 Providing the fact that the polymer would have an almost full transmission at the emission wavelength,
126 a scintillator – and therefore its fluorophores – with a very large Stokes shift should virtually not display
127 any self-absorption process. Thus, self-absorption depends on both the volume and the concentration
128 of the secondary fluorophore in a ternary organic scintillator. To the best of our knowledge, only one
129 article relates the dependence between the secondary fluorophore concentration with the volume.
130 Adadurov *et al.* adjusted the weight percentage of the secondary fluorophore to the volume of the
131 material.⁹ Thanks to beta spectroscopy, the authors determined a relationship between scintillation
132 efficiency and weight concentration of POPOP, used as the secondary fluorophore. Furthermore, they
133 drew the weight concentration of the secondary fluorophore relative to the optical length.
134 Our aim is to understand the influence of the secondary fluorophore in neutron/gamma discrimination
135 process. According to the mentioned literature, self-absorption taking place in lab-made ternary
136 systems could be a consequence of the choice of the secondary fluorophore and its concentration. Our
137 strategy is to evaluate the neutron/gamma discrimination abilities of plastic scintillators of different
138 sizes and various secondary fluorophores, incorporated at two weight concentrations. This would
139 enable us to highlight the self-absorption phenomenon.

140

141 II. EXPERIMENTAL

142 All the chemicals were purchased from Sigma-Aldrich and used as received unless otherwise stated.
143 Styrene was vacuum-distilled over calcium hydride prior to the experiment and the inhibitors were
144 removed from the cross-linker agent.

145 The general procedure for the plastic scintillator preparation is as follows: in a flame-dried round
146 bottom flask filled with argon, the powders were dissolved in the liquids. The gases were then removed
147 using the freeze-pump-thaw technique, and the solution was carefully transferred into a vial for radical
148 polymerization. After completion, the vial was shattered with a mallet and the scintillator was obtained
149 after shaping and polishing the raw material. The contours and back were ultimately covered with PTFE
150 for better light collection through multiple diffusive reflections.

151 Pulse Shape Discrimination was performed by irradiating plastic scintillators with a ^{252}Cf radioactive
152 source, whose activity was 560 kBq at the time of measurement. The tested scintillator was coupled
153 to the photocathode of a Hamamatsu H11284-MOD Photomultiplier Tube¹⁰ with Rhodorsil RTV141A
154 optical grease. The PMT was fed by a CAEN N1470 high voltage operating at -1500 V. The anode of the
155 PMT was linked to a CAEN DT5743 digitizer, whose bandwidth, sampling rate and resolution are
156 500 MHz, 800 MS/s and 12 bits, respectively. The WaveCatcher software from CAEN was used to
157 record 25,000 pulses (or 35,000 pulses in some cases) with an integration time equal to 1280 ns. The

158 charge comparison method was then applied off-line thanks to a Matlab lab-made algorithm. It
159 calculates delayed and total areas under each pulse, displays the bi-dimensional diagram and evaluates
160 the Figure of Merit.

161 Gamma spectra were recorded using the same setup experiment: the CAEN DT5743 electronic board
162 connected to the Hamamatsu H11284-MOD Photomultiplier tube. A 9.75 MBq ^{22}Na source was placed
163 2.5 cm away from the top of the plastic scintillator to be analyzed.

164 Liquid scintillators were contained in 3 cm³ quartz cuvettes. The solvent was spectroscopic toluene,
165 and 0.03 wt% secondary fluorophore (POPOP, dimethylPOPOP, 9,10-DPA or bis-MSB) was introduced.
166 Fluorescence spectra were recorded at 90° from the excitation light (270 nm) with a Horiba Jobin Yvon
167 Fluoromax-4P device, monitored with FluorEssence software.

168

169 III. NATURE OF THE SECONDARY FLUOROPHORE AND ITS IMPACT ON NEUTRON/GAMMA DISCRIMINATION

170 1. *Experimental details*

171 As already said in the introduction, a plastic scintillator is generally a ternary system. For the purpose
172 of the studies, ternary plastic scintillators were lab-made according to a previous preparation.¹¹ The
173 first series consists in eight plastic scintillators of 12 mm diameter and 120 mm height, thus giving a
174 14 cm³ volume. The matrix and the primary fluorophore are identical: the matrix is a cross-linked
175 polystyrene derivative and the weight concentration of the first solute (biphenyl) is 17 wt%. Four
176 different secondary fluorophores were added as well to the scintillator mixture, with two different
177 weight concentrations: 0.1 and 0.2 wt%, respectively. The list of lab-made scintillators is presented in
178 Table 1, with the structure of the molecules in the Figure 1. The name of these plastics relies on the
179 nature of the secondary fluorophore (in summarized form) and the weight concentration at which it is
180 added.

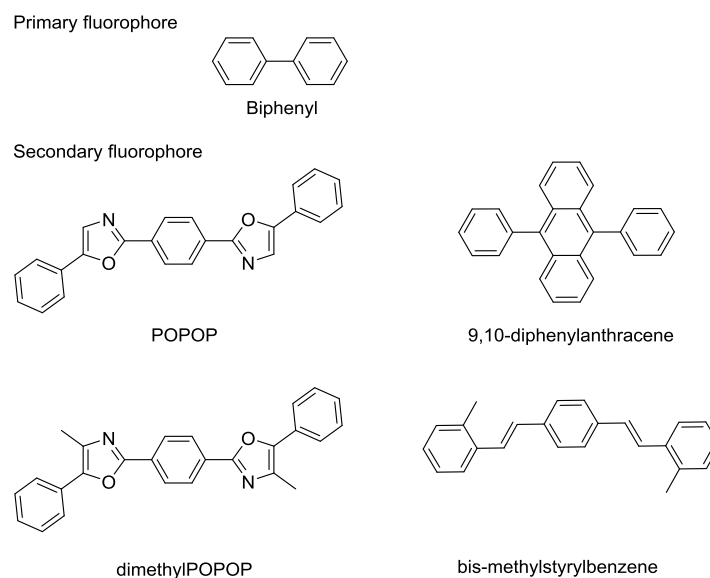
181

182 *Table 1. Lab-made plastic scintillators (∅ 12 mm × h 120 mm) prepared to study the influence of the nature of the secondary*
183 *fluorophore*

Scintillator	Secondary fluorophore	Concentration (wt%)
Bis1	Bis-MSB	0.1
Bis2	Bis-MSB	0.2
DPA1	9,10-DPA	0.1
DPA2	9,10-DPA	0.2
DMP1	DiMePOPOP	0.1
DMP2	DiMePOPOP	0.2
P1	POPOP	0.1

P2	POPOP	0.2
----	-------	-----

184



185

186

187

Figure 1. Chemical structures of biphenyl, 1,4-bis(5-phenyl-2-oxazolyl)benzene, 9,10-diphenylanthracene, 1,4-bis-2-(4-methyl-5-phenyloxazolyl)benzene and bis-methylstyrylbenzene.

188

189 The pulses assigned to neutrons were sorted, averaged and four photophysical criteria were evaluated
 190 thanks to the fitting module of the Igor Pro software: fast and slow decay times and their related
 191 intensities. Equation 3 displays the formula of the slow relative intensity, and Equation 4 shows the
 192 relationship between fast and slow relative intensities.

193 Equation 3

$$I_{rel,s} = \frac{A_{0s}\tau_s}{A_{0s}\tau_s + A_{0f}\tau_f}$$

194

195

196 Equation 4

$$I_{rel,s} + I_{rel,f} = 1$$

197

198

199 A_{0f} and A_{0s} stand for fast and slow intensities at $t = 0$ of the mean neutron signal, and τ_f and τ_s are
 200 the fast and slow decay times, respectively, which are convolved with the transit time of the PMT
 201 (equal to 29 ns according to the H11284-MOD PMT datasheet¹⁰).

202 Unlike commercial data sheets of organic scintillators that describe the decay time of a scintillator with
 203 three components,¹² we only evaluate fast and slow components of the signal. In fact, we consider
 204 that the fast component corresponds to prompt fluorescence – it is the decay rate of the fluorescence
 205 deactivation of singlet excited states – and the slow one represents delayed fluorescence, which is the
 206 radiative deactivation of the triplet excited states thanks to Triplet-Triplet Annihilation (TTA) mainly.

207 This photophysical phenomenon is the key step to explain fast neutron/gamma discrimination in such
208 scintillators.¹³

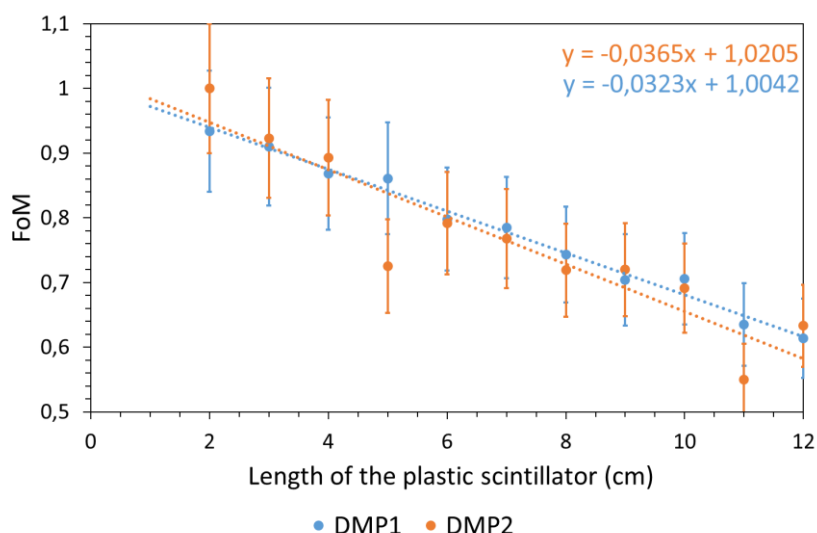
209

210 2. Results

211 1) Self-absorption in 12 mm × 120 mm scintillators

212 Before testing all scintillators presented in Table 1, we focused on neutron/gamma discrimination
213 abilities of DMP1 and DMP2 containing dimethylPOPOP as the secondary fluorophore. Our goal was
214 to study and highlight self-absorption in these long and small plastic scintillators. Thus, plastics were
215 irradiated with the ²⁵²Cf radioactive source introduced above. We obtained FoM values thanks to
216 signal processing. We then cut centimeter by centimeter both plastic materials and listed their FoM
217 value after each removal. Results are showed in Figure 2.

218



219

220 *Figure 2. Evolution of FoM of DMP1 (0.1 wt% DiMePOPOP) and DMP2 (0.2 wt% DiMePOPOP) plastic scintillators along with*
221 *the length of scintillators (note that these materials were not from the same batch as the ones tested in Table 1).*

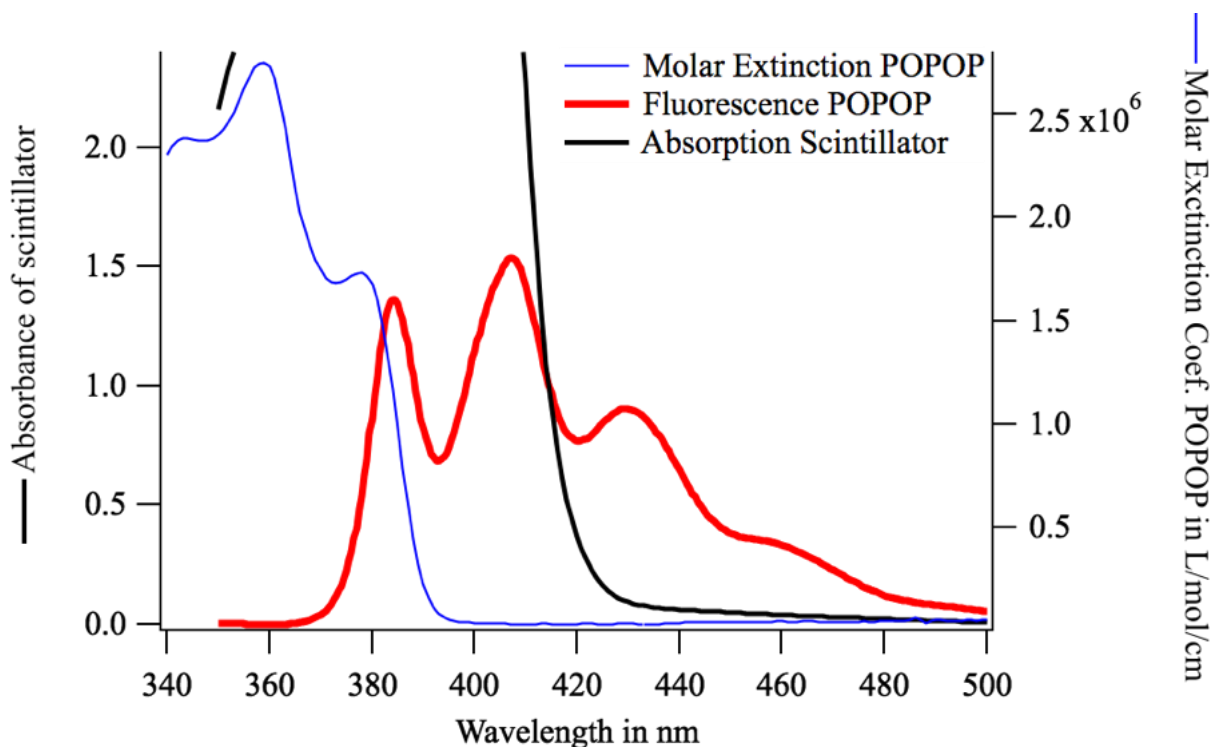
222

223 We noticed that the longer the samples, the smaller the FoM values. Furthermore, the FoM value is
224 linearly proportional to the length of the plastic scintillator, whatever the weight concentration of the
225 secondary fluorophore – at least in this study. The mean relative loss of FoM is around 55 %, so both
226 plastic scintillators lose more than twice their neutron/gamma discrimination abilities from 2 to 12 cm
227 long. Finally, linear fits, for which equations are written on Figure 2, indicate that the weight
228 concentration of DiMePOPOP influences FoM as well.

229 In the case of POPOP, self-absorption of POPOP by the scintillator can be predicted from the absorption
230 and fluorescence spectra of this molecule in the scintillator. On Figure 3 the absorption of a thin POPOP
231 solution and the one of a 8.3 cm long scintillator are compared with the fluorescence of POPOP.

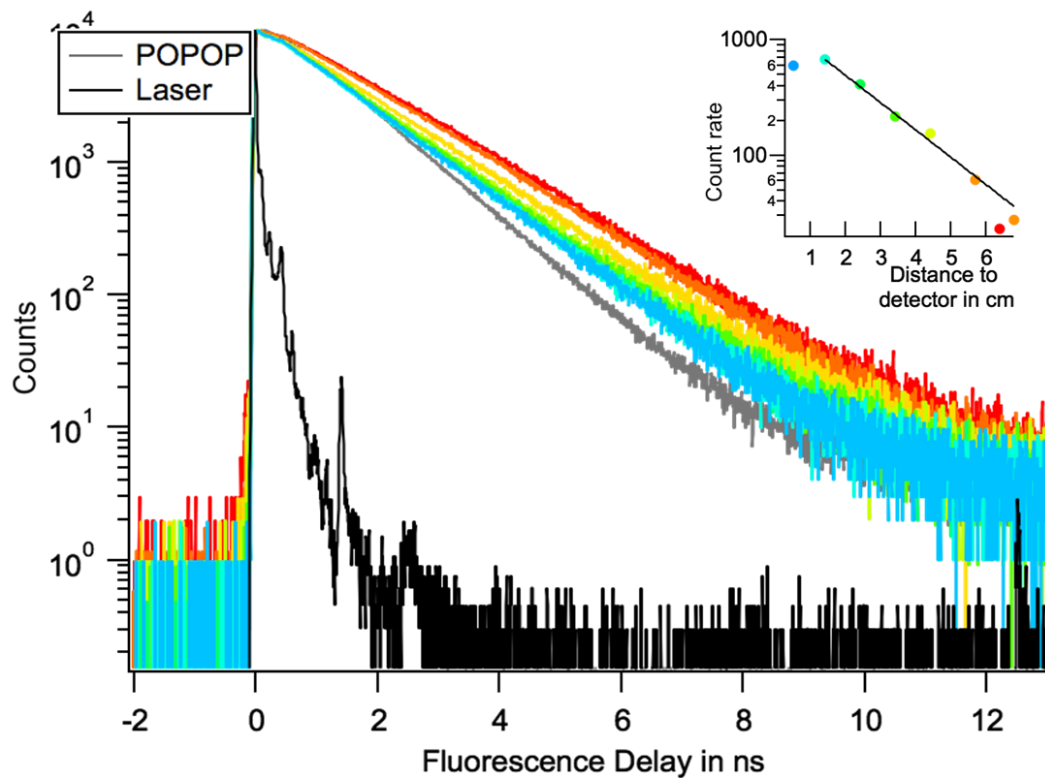
232 Whereas in solution only the first fluorescence peak at 382 nm is re-absorbed, in a thick scintillator the
 233 second peak at 408 nm is impacted. This has two consequences on the collection of fluorescence and
 234 on its apparent lifetime (Figure 4). The same PTFE-wrapped scintillator was excited with a 390 nm laser.
 235 Less than 10 % of the light produced 6 cm away from the head reached the detector. Due to multiple
 236 absorptions and re-emission, the apparent fluorescence decay time was increased by 50 %. We can
 237 thus qualitatively conclude that the self-absorption process can affect the FoM value in those long and
 238 small sized plastic scintillators.

239



240
 241 *Figure 3. Absorption (blue) and fluorescence (red) spectra of POPOP in cyclohexane from*
 242 *<https://omlc.org/spectra/PhotochemCAD/html/077.html> compared to the absorption spectrum of a 8.3 cm long scintillator*
 243 *with 0.2 wt% POPOP. The red shift observed in the absorption of the scintillator compared to the diluted POPOP is due to the*
 244 *high concentration ($5 \cdot 10^{-3}$ mol/L) of POPOP in the scintillator. A significant part of the fluorescence is reabsorbed.*

245



246

247 *Figure 4. Photoluminescence decay time of the scintillator when excited at various distances from the detector head.*

248

249 *2) Influence of the nature of the secondary fluorophore in neutron/gamma discrimination abilities of plastic*
 250 *samples*

251 Lab-made plastic scintillators presented in Table 1 were tested under neutron and gamma rays
 252 irradiation thanks to the protocol described above. Fast and slow decays, and the slow relative
 253 intensity of each material are listed in Table 2. We already noticed that the FoM value depends on the
 254 weight concentration of the secondary fluorophore. When one compares the discriminating efficiency
 255 of scintillators loaded with a specific weight concentration of secondary fluorophore, one notices that
 256 FoM values are distinct, even considering the associated uncertainty. Besides, we deliberately
 257 maximized the total uncertainty associated to the FoM measurement. Therefore, it includes the
 258 precision and accuracy errors of the whole detection system, as well as the repeatability and
 259 reproducibility uncertainties. Then, the weight concentration also influences the FoM value: when it is
 260 0.2 wt%, FoM increases, except for bis-MSB scintillators. Fast decay times display relatively close
 261 values, whereas slow decay times extend from 86 ns up to 126 ns for DMP2 and DPA2, respectively.
 262 Furthermore, the slow decay component of Bis2 have not been evaluated because of an unreliable fit:
 263 it does not satisfy our fitting criterion, which was in our case $\chi^2 > 0.99$.

264 According to these results, there is a correlation between the FoM value and the slow relative intensity
 265 and the slow decay time. Thus, it is not sufficient to have a secondary fluorophore with a slow decay

266 time like bis-MSB or 9,10-DPA (around a hundred of ns here) but the tail proportion, which would
 267 represent the triplet-triplet annihilation, has to be high enough.

268

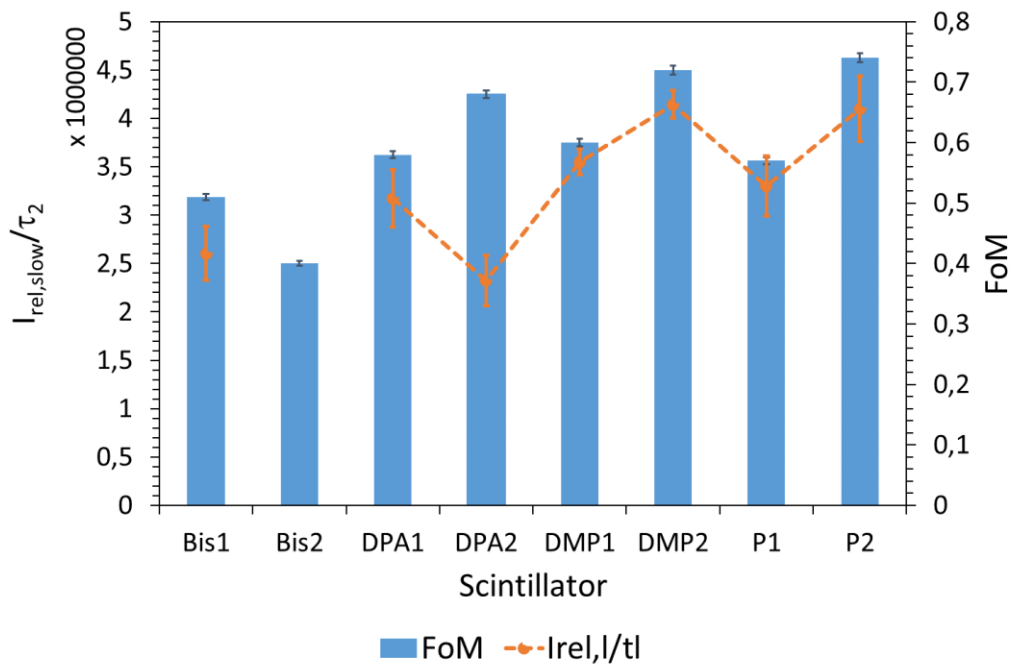
269 *Table 2. Fast neutrons/gamma discrimination results (in terms of FoM value) for plastic scintillators (\varnothing 12 mm \times h 120 mm)*
 270 *presented in Table 1.*

Scintillator	τ_f (ns)	τ_s (ns)	Slow relative intensity	FoM
Bis1	11.51 ± 0.11	115 ± 15	0.30	0.51 ± 0.05
Bis2	11.52 ± 0.13	Unreliable fit	n.d.	0.44 ± 0.04
DPA1	17.78 ± 0.19	103 ± 11	0.26	0.58 ± 0.06
DPA2	15.82 ± 0.17	126 ± 11	0.29	0.68 ± 0.07
DMP1	11.59 ± 0.05	88.9 ± 4	0.32	0.60 ± 0.06
DMP2	10.16 ± 0.05	86.2 ± 3.7	0.36	0.72 ± 0.07
P1	11.15 ± 0.12	89.8 ± 9	0.30	0.57 ± 0.06
P2	10.73 ± 0.16	99.7 ± 12	0.41	0.74 ± 0.07

271

272 If we calculate the ratio of the slow relative intensity and the slow decay time for each tested
 273 scintillator, we notice that it follows the FoM trend except for DPA2. Thus, this new criterion measures
 274 the efficiency of delayed fluorescence, which is directly correlated to the FoM value. This observation
 275 agrees with the results obtained by Dalla Palma *et al.*,¹⁴ who have experimentally observed that the
 276 FoM value depends on two parameters. On one side, the light yield is responsible of differences in FoM
 277 values, especially at low energies. On the other side, the numerator of Equation 3 is a function of the
 278 slow decay intensity. According to our results presented in Figure 5, it should be the ratio of this slow
 279 intensity and the slow decay time.

280



281

282 *Figure 5. Ratio of the slow relative intensity and the slow decay time depending on the FoM value for each scintillator.*

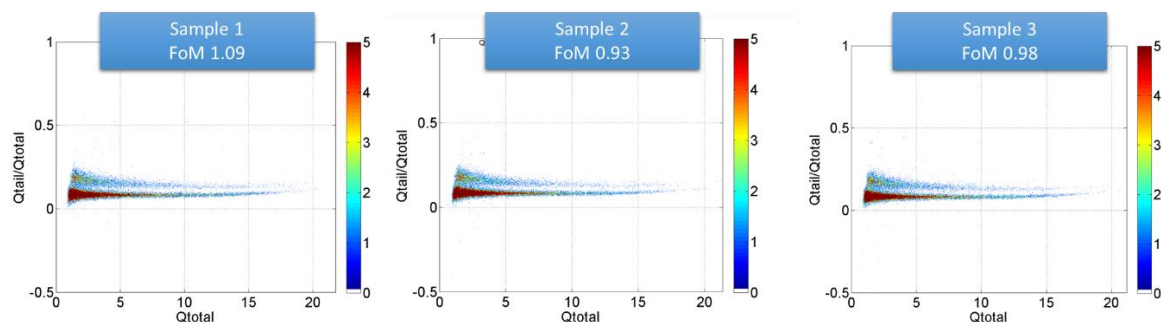
283

284 As suspected, the secondary fluorophore plays a role outside its primary role of wavelength shifter. It
 285 influences the plastic's neutron/gamma discrimination abilities, it lengthens the short-lived decay and
 286 it changes the delayed luminescence intensity. The lengthening of the short-lived decay is due to self-
 287 absorption process, which occurs even in medium size scintillators (12 cm length in our experiment).
 288 In addition to self-absorption, it is important to check about the scale-up of the material. Thermally
 289 initiated polymerization may lead to bulk materials with cracks, bubbles or colored centers, especially
 290 for large-size scintillators.

291 To confirm the good homogeneity of PSD-plastics, two other experiments were also performed, where
 292 three identical pieces were randomly cut from a bigger scintillator, and another thin-and-long
 293 scintillator was cut into four identical pieces, which were benchmarked. The first series was to evaluate
 294 the homogeneity of large scintillators. From a 10 cm height and 7 cm diameter scintillator, three pieces
 295 were isolated at the same size and volume, which is 2 cm height and 2.7 cm diameter. At first, their
 296 light output was evaluated using a ^{22}Na source. A 17% light output difference was observed between
 297 the best and worst scintillator. Then they were strictly compared in terms of fast neutrons/gamma
 298 discrimination. Figure 6 gives the n/ γ discrimination results of the three samples. Homogeneity
 299 problems are dismissed as a potential explanation for the lack of discrimination in large-scale plastic
 300 scintillators.

301 In the second series testing homogeneity, an 8 cm long and 1.8 cm diameter scintillator was cut in four
302 2 cm long samples. Whereas the four small samples showed an almost identical FoM value (0.80, 0.77,
303 0.80 and 0.74 in the range 500 – 1000 keVee), a dramatic decrease of the FoM was observed for the
304 full scintillator, with a value of 0.56 only in the same range of energy. The deviation of the gamma
305 spectra was 5.8 % only, therefore claiming a good light output uniformity between the samples. This
306 factor is not the one affecting the FoM decrease with the length of the scintillator.

307



308

309 *Figure 6. Biparametric spectra and FoM values for 3 randomly cut samples from a bigger monolith.*

310

311 3. *Exciplex formation*

312 Beyond reabsorption effects, the secondary fluorophore interacts with the excited state dynamics in
313 the scintillator. If acting only as a wavelength shifter the pulse shapes should reflect the biphenyl
314 excited state dynamics. The pulse shape should be the same whatever the nature of the secondary
315 fluorophore. The differences in the slow component lifetime and fraction that are measured show that
316 the secondary fluorophore plays a role in the excited states nature and dynamics. The slow component
317 is attributed to the triplet-triplet annihilation. In this context, we want to identify the interaction of
318 the triplet state of biphenyl with that of the secondary fluorophore. Herein, only the case of POPOP
319 was studied.

320 We believe that biphenyl excited states can interact with the secondary fluorophore in two ways:

- 321 - Formation of exciplexes (excimers between at least two different molecules),
- 322 - Triplet energy transfers between the primary and the secondary fluorophores.

323 For this experiment, we reproduced the chemical composition of standard lab-made plastic
324 scintillators in the liquid state, and we tested these liquid scintillators by emission spectroscopy. In a
325 few words, exciplexes and excimers are molecular associates, which exist only in excited states, singlet
326 or triplet states according to the excited state of the donor. Their detection is only possible from
327 emission spectroscopy.¹⁵

328

329 1) *Exciplex formation*

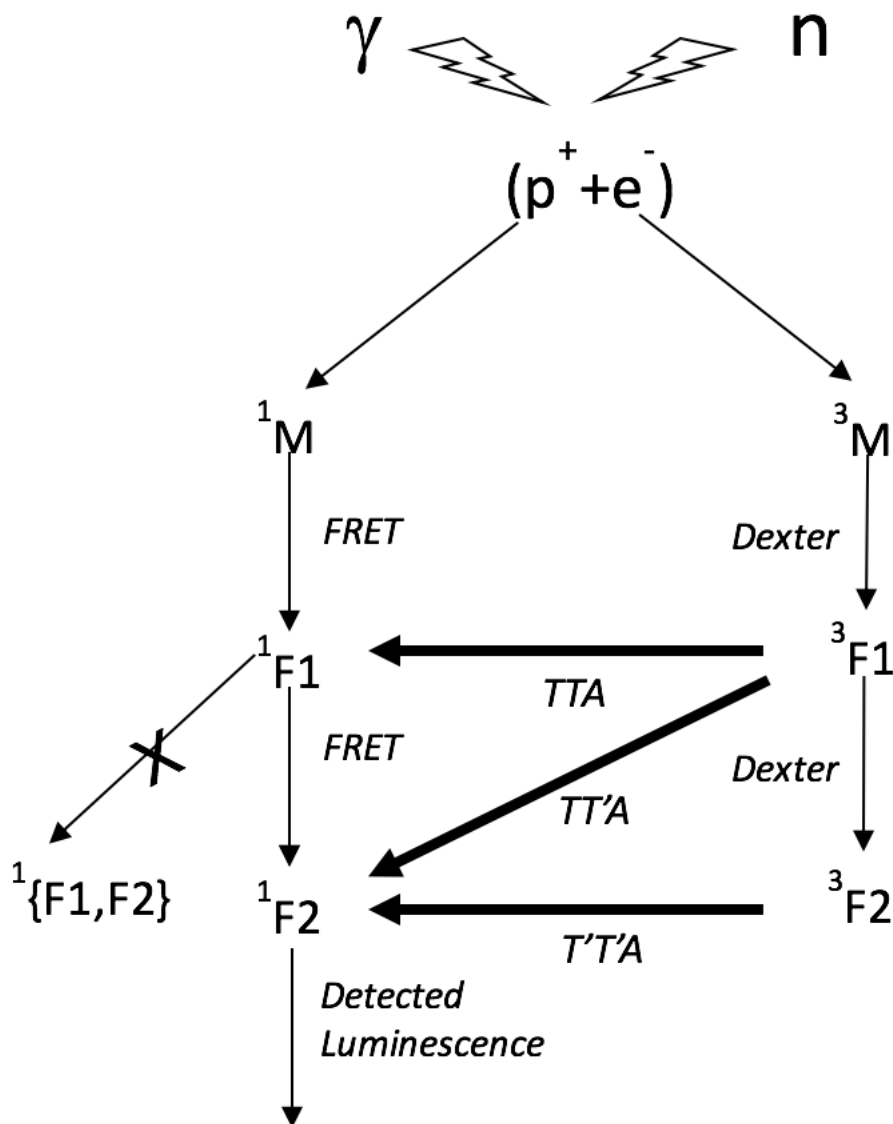
330 The spectroscopy experiment is carried out in several conditions:

- 331 - The cuvette containing the secondary fluorophore in toluene is put into open air,
- 332 - The same cuvette is continuously degassed with argon,
- 333 - 15 wt% of biphenyl is added to the liquid scintillator. Similarly, the cuvette is put under air and
334 argon.

335 Whatever the studied conditions, there was no significant difference in the shape and amplitude of
336 the emission spectra. We therefore assume that no exciplexes – {primary fluorophore – secondary
337 fluorophore} or {secondary fluorophore – secondary fluorophore} – were created.

338 The Figure 7 presents the deactivation pathways of the excitation energy in a ternary organic
339 scintillator. After the ionization by neutrons or gamma rays, the charge recombination creates excited
340 state of the matrix. This excitation is transferred to the primary and secondary fluorophores by FRET
341 or Dexter energy transfer. In the neutron-induced traces, the high linear density of charges allows non-
342 geminated recombinations and the formation of triplet excited states. The presence of these triplet
343 states is revealed by the delayed luminescence following the triplet-triplet annihilation of densely
344 excited traces. It is seen that the triplet of the secondary fluorophore is also produced and contributes
345 as well to the delayed luminescence.

346



347

348 *Figure 7. Deactivation pathways of the excitation energy in a ternary organic scintillator. Matrix: M, primary fluorophore: F1*
 349 *and secondary fluorophore: F2.*

350

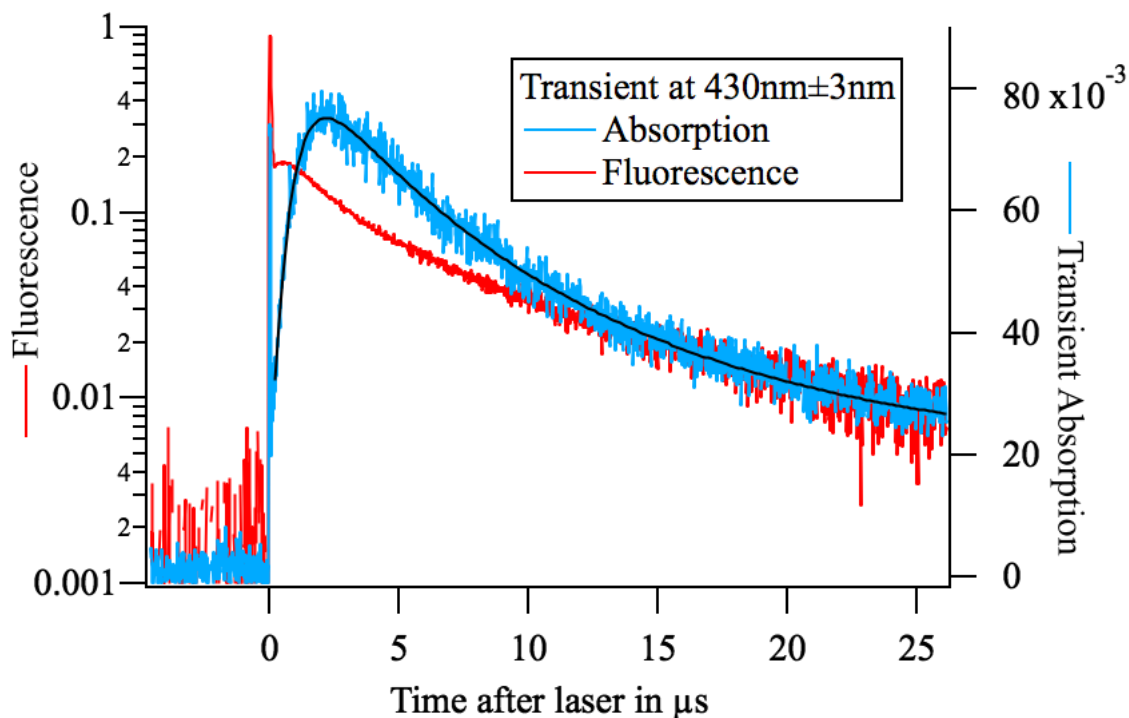
351 2) *Triplet energy transfers*

352 Triplet state decay times were recorded thanks to a transient absorption experiment. A Nd:YAG laser
 353 was used to produce 5 ns pulses. KDP crystals allowed us to quadruple the frequency, thus exciting at
 354 the wavelength $\lambda = 266$ nm. The liquid sample, contained in a 1 cm thick quartz cuvette, was excited
 355 with an incident energy of 3 mJ per pulse. Two solutions were studied:

- 356 - A = a liquid sample composed with cyclohexane as the matrix, containing $1.46 \cdot 10^{-3}$ mol.L⁻¹ biphenyl,
- 357 - B = the same A solution plus $2 \cdot 10^{-4}$ mol.L⁻¹ POPOP (close to saturation).

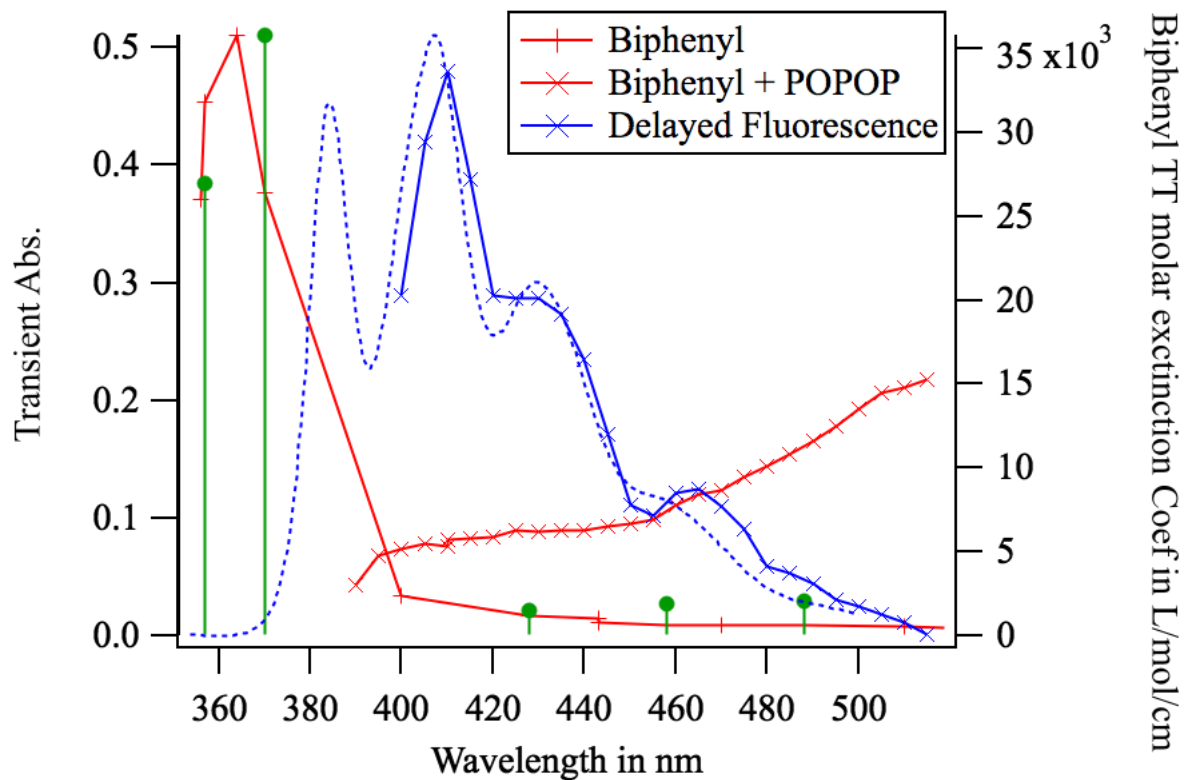
358 In cyclohexane, the laser excitation at 266 nm is absorbed by the biphenyl over a depth of 1 cm. Both
 359 transient fluorescence and absorption are recorded; Figure 8 shows the transient absorption and

360 fluorescence spectroscopy of solution B. Its prompt fluorescence is observed at 430 nm and is followed
361 by a delayed luminescence. The transient absorption at 430 nm rises and reaches a maximum after
362 2.5 μs before decaying. Both transient signals can be identified by their spectra from 380 to 520 nm in
363 Figure 9.



364
365 *Figure 8. Transient fluorescence (red) and absorption (blue) spectra of solution B made of biphenyl and POPOP in cyclohexane*
366 *after excitation in the Biphenyl absorption band at 266 nm. Both the prompt and the delayed fluorescence are observed. The*
367 *POPOP triplet population rises in 2.5 μs from the Biphenyl triplet population.*

368
369 The delayed fluorescence spectrum of solution B (Blue x in Figure 9) shows a major contribution of the
370 POPOP molecule. If one considers the transient absorption spectra, the one of sample A (Red + in
371 Figure 9) shows the influence of biphenyl with a maximum at 370 nm as reported in the literature,¹⁶
372 whereas the one of sample B (Red x in Figure 9) displays the contribution of POPOP. The global
373 maximum stands at around 500 – 520 nm. Pavlopoulos *et al.* already observed a similar spectrum, and
374 assigned it to the absorption spectrum of the triplet state of POPOP.¹⁷ The rise time of the triplet of
375 POPOP is 0.7 μs for a concentration of $2 \cdot 10^{-4} \text{ mol} \cdot \text{L}^{-1}$. This corresponds to a transfer rate of $7 \cdot 10^9 \text{ s}^{-1}$,
376 that is close to the diffusion-limited rate. In presence of POPOP, the triplet state of biphenyl transfers
377 to POPOP at any collision.
378

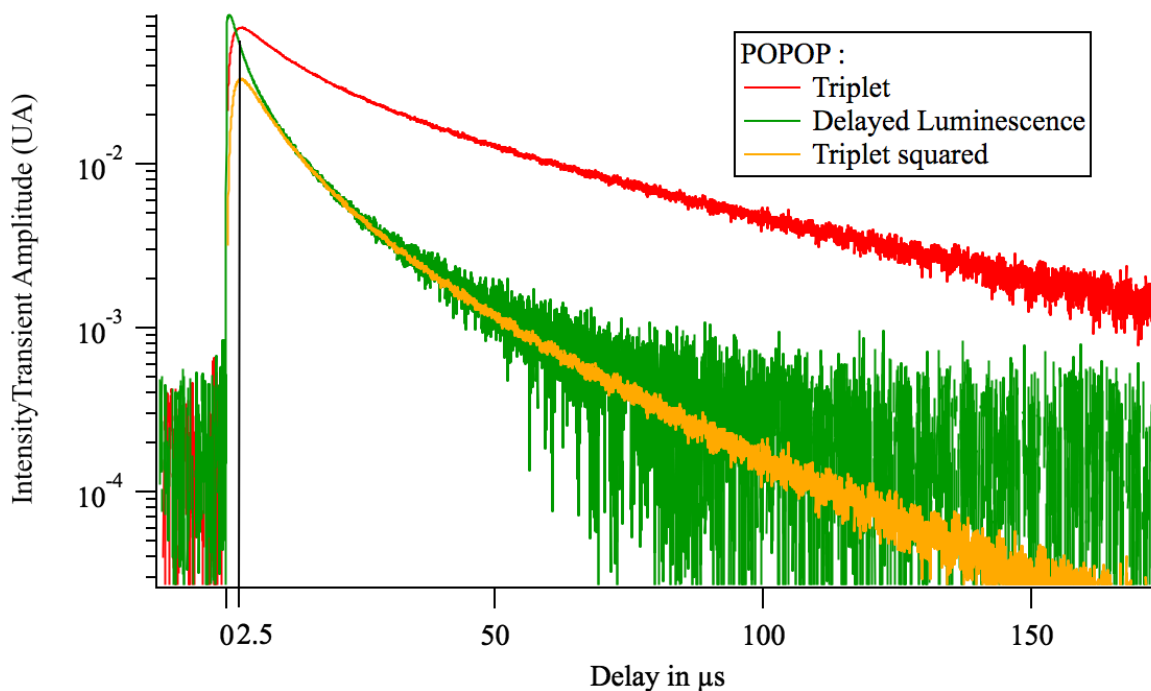


379

380 *Figure 9. Transient absorption spectra of biphenyl in sample A compares with the published spectrum of biphenyl's triplet*
 381 *(green dots). The transient spectrum of solution B biphenyl + POPOP shows the transfer of triplet state from biphenyl towards*
 382 *POPOP. The delayed fluorescence of POPOP spectrum is compared to the prompt fluorescence one (blue dashed line).*

383

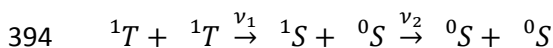
384 The kinetics of both the POPOP delayed fluorescence and POPOP triplet states are analyzed in Figure
 385 10, which shows that the delayed fluorescence comes from the annihilation of triplet of POPOP
 386 through a bimolecular process. Beyond 10 μ s the delayed fluorescence decays as the square of the
 387 POPOP triplet concentration as expected for triplet-triplet annihilation process. At shorter times, the
 388 triplet of biphenyl is present and contributes to the delayed luminescence.



389
 390 *Figure 10. POPOP triplet photoluminescence decay (red), delayed luminescence (green), and squared triplet (orange).*

391
 392 As a reminder, the triplet-triplet annihilation process is written as:

393 *Equation 5*



395 The rate ν_1 is then:

396 *Equation 6*

$$397 \quad \nu_1 = k_1 [{}^1T]^2$$

398 The emission of the fluorescence photon is fast (1.2 ns) compared to the triplet-triplet annihilation
 399 (μs), then:

400 *Equation 7*

$$401 \quad \nu_1 = \nu_2 = k_1 [{}^1T]^2$$

402 By definition, ν_2 refers to a quantity of photons emitted by delayed fluorescence per second, thus
 403 corresponds to the delayed fluorescence intensity. According to Equation 7, the intensity of delayed
 404 fluorescence is proportional to the square of the excited triplet states concentration in the case of a
 405 triplet-triplet annihilation. This is observed in Figure 10, where the tail of the delayed fluorescence is
 406 proportional to the square of the POPOP triplet concentration. At shorter times, more fluorescence is
 407 observed. However, at times shorter than $2.5 \mu\text{s}$ a rise of POPOP triplet is seen; biphenyl triplet states
 408 are present and they contribute to the delayed fluorescence as well. In conclusion, POPOP triplet is
 409 present in solution B and triplet-triplet annihilation of POPOP takes place in the liquid sample. At

410 shorter times TTA between two molecules of the primary fluorophore or between excited molecules
411 of the primary fluorophore and of the secondary fluorophore do occur. In a solid matrix, the triplet of
412 POPOP is trapped because the distance between POPOP molecules (1 nm) is too high to allow hopping.
413 However, the triplet of biphenyl is mobile, which allows biphenyl-biphenyl TTA and biphenyl-POPOP
414 TTA to occur.

415

416

IV. DISCUSSION

417

418 Our work relates the influence of the secondary fluorophore in a ternary plastic scintillator aiming at
419 discriminating fast neutrons from gamma rays. Thanks to neutron/gamma experiments, we showed
420 that the length of POPOP-based plastic scintillators in the range (\varnothing 12 mm \times h 120 mm) influences
421 negatively the discrimination abilities. We have shown that this is not due to preparation issues where
422 large plastic might be heterogeneous in composition. As self-absorption relies on the spectral overlap
423 between the absorption and the emission spectra of the secondary fluorophore (in a ternary system),
424 we highlight the influence of this fluorophore on neutron/gamma discrimination abilities of the plastic
425 sample. The mean relative loss of FoM is 55 %.

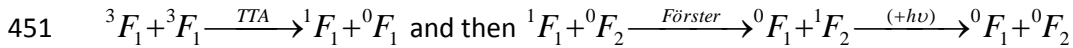
426

427 We have shown that scintillators with the same quantity of primary fluorophore, irradiated under the
428 same conditions have different FOM depending on the nature of the secondary fluorophore. The FoM
429 values are quite different despite the identical measurement protocol: it varies from 0.44 for the worse
430 discriminating scintillator (Bis2) to 0.74 for the best one (P2). We have checked if the FoM difference
431 does not come from exciplexes between the primary and the secondary fluorophore in liquid mixtures.
432 Since no exciplex was created in our liquid system (at least with our experimental conditions), we
433 assume that no exciplexes are formed in plastics as well. Thanks to transient absorption experiments,
434 the formation of POPOP triplets was observed when biphenyl was excited. For the first time, the
435 existence of a delayed POPOP luminescence coming from the triplet-triplet annihilation of POPOP was
436 observed as well in a liquid sample. In solid samples, we then assumed that TTA also takes place in
437 plastic scintillators, as well as in liquids. For now, transient absorption measurements have not
438 assessed with accuracy the nature of the involved molecules in the TTA process.

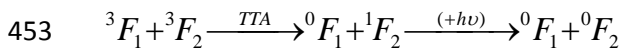
439 Equations 8 and 9 give the energetic transfers that we observed thanks to transient absorption
440 experiments. This explains the influence of the secondary fluorophore in neutron/gamma
441 discrimination. Equation 8 formalizes the TTA process between two excited triplet states of the primary
442 fluorophore followed by a Förster energy transfer of the resulting excited singlet state of the primary
443 fluorophore towards the secondary fluorophore. Equation 9 relates to a crossed TTA, that is to say

444 between the excited triplet states of the primary and the secondary fluorophores. These two equations
445 require a diffusion of the biphenyl triplets that can be achieved in solids sample thanks to a hopping
446 of the triplets between biphenyl neighbors. This is in good agreement with the huge increase of
447 primary fluorophores concentration necessary to reach a visible PSD in plastics,³ along with the
448 observation that plastics loaded with 0.2 wt% secondary fluorophores give better FoM values than
449 0.1 wt% ones, at least with our global formulation suitable for n/γ PSD (this work).

450 *Equation 8*



452 *Equation 9*



454

455

456

V. CONCLUSION

457

458 Plastic scintillators aiming at discriminating fast neutrons from gamma rays suffer from a decrease of
459 their performances while increasing their volume. It was proven that fabrication process does not lead
460 to heterogeneous materials, so our main hypothesis is that self-absorption is the main nefarious effect.
461 In particular, the nature and the concentration of the secondary fluorophore have a strong influence
462 on the n/γ discrimination ability, as confirmed from the study of four different molecules. Preliminary
463 experiments seem to highlight specific energy transfers between primary and secondary fluorophores.
464 Future work will consist in assigning probabilities of each transfer, which means evaluating reaction
465 rate constants.

466

467

VI. ACKNOWLEDGEMENTS

468

469 We are indebted to the French National Agency "ANR" for financial support, within the frame of the
470 Nesynded project (ANR-15-CE39-0006).

471

VII. REFERENCES

-
- ¹ R.T. Kouzes, J.H. Ely, L.E. Erikson, W.J. Kernan, A.T. Lintereur, E.R. Siciliano, D.L. Stephens, D.C. Stromswold, R.M. Van Ginhoven, M.L. Woodring, Neutron detection alternatives to ³He for national security applications, *Nucl. Instr. Methods A*, 623 (2010) 1035-1045.
- ² P. Peerani, A. Tomanin, S. Pozzi, J. Dolan, E. Miller, M. Flaska, M. Battaglieri, R. De Vita, L. Ficini, G. Ottonello, G. Ricco, G. Dermody, C. Giles, Testing on novel neutron detectors as alternative to ³He for security applications, *Nucl. Instr. Methods A*, 696 (2012) 110-120.
- ³ G.H.V. Bertrand, M. Hamel, F. Sguerra, Current Status on Plastic Scintillators Modifications, *Chem. – Eur. J.*, 20 (2014) 15660-15685.
- ⁴ J. Kalyna, I.J. Taylor, Pulse shape discrimination: an investigation of n-γ discrimination with respect to size of liquid scintillator, *Nucl. Instr. Methods*, 88 (1970) 277-287.
- ⁵ B. Sipp, J.A. Miehe, Fluorescence self-absorption effect and time resolution in scintillation counters, *Nucl. Instr. Methods*, 114 (1974) 255-262.
- ⁶ M. Moszyński, B. Bengtson, Light pulse shapes from plastic scintillators, *Nucl. Instr. Methods*, 142 (1977) 417-434.
- ⁷ N.P. Zaitseva, A.M. Glenn, A.N. Mabe, M.L. Carman, C.R. Hurlbut, J.W. Inman, S.A. Payne, Recent developments in plastic scintillators with pulse shape discrimination, *Nucl. Instr. Methods A*, 889 (2018) 97-104.
- ⁸ E. Montbarbon, M.-N. Amiot, D. Tromson, S. Gaillard, C. Frangville, R. Woo, G.H.V. Bertrand, R.B. Pansu, J.-L. Renaud, M. Hamel, Large irradiation doses can improve the fast neutron/gamma discriminating capability of plastic scintillators, *Phys. Chem. Chem. Phys.*, 19 (2017) 28105-28115.
- ⁹ A.F. Adadurov, P.N. Zhmurin, V.N. Lebedev, V.D. Titskaya, Optimizing concentration of shifter additive for plastic scintillators of different size, *Nucl. Instr. Methods A*, 599 (2009) 167-170.
- ¹⁰ Hamamatsu H11284-MOD (R7724-100 photocathode): <https://www.hamamatsu.com/jp/en/R7724.html>.
- ¹¹ P. Blanc, M. Hamel, C. Dehé-Pittance, L. Rocha, R.B. Pansu, S. Normand, Neutron/gamma pulse shape discrimination in plastic scintillators: preparation and characterization of various compositions, *Nucl. Instr. Methods A*, 750 (2014) 1-11.
- ¹² Eljen Technology EJ-276 PSD Plastic Scintillator: <https://eljentechnology.com/products/plastic-scintillators/ej-276>.
- ¹³ R. Voltz, G. Laustriat, Radioluminescence des milieux organiques I. Étude cinétique, *J. Phys. France*, 29 (1968) 159-166.
- ¹⁴ M. Dalla Palma, T. Marchi, S. Carturan, C. Checchia, G. Collazuol, F. Gramegna, N. Daldosso, V. Paterlini, A. Quaranta, M. Cinausero, M. Degerlier, Pulse Shape Discrimination in Polysiloxane-Based Liquid Scintillator, *IEEE Trans. Nucl. Sci.*, 63 (2016) 1608-1615.
- ¹⁵ T. Förster, Excimers, *Angew. Chemie Int. Ed.*, 8 (1969) 333-343.
- ¹⁶ D. Lavalette, C. Tetreau, Triplet-triplet absorption of biphenyl and related compounds. *Chem. Phys. Lett.* 29 (1974) 204-209.
- ¹⁷ T.G. Pavlopoulos, P.R. Hammond, Spectroscopic Studies of Some Laser Dyes, *J. Am. Chem. Soc.*, 96 (1974) 6568-6579.